Environmental Pollution 244 (2019) 174–181

Contents lists available at ScienceDirect

Environmental Pollution

journal homepage: www.elsevier.com/locate/envpol

Mechanism of uranium release from uranium mill tailings under long-term exposure to simulated acid rain: Geochemical evidence and environmental implication☆

Meiling Yin [a, 1], Jing Sun [b, 1], Yongheng Chen [a], Jin Wang [a, c, d, *], Jianying Shang [e], Nick Belshaw [d], ChuanChou Shen [f, g], Juan Liu [a, d, **], Huosheng Li [a], Wensheng Linghu [h], Tangfu Xiao [a], Xinjiao Dong [i], Gang Song [a, c], Enzong Xiao [a], Diyun Chen [a, c]

[a] School of Environmental Science and Engineering, Guangzhou University, Guangzhou, 510006, China
[b] School of Earth Sciences, University of Western Australia, Perth, WA, 6009, Australia
[c] Guangdong Provincial Key Laboratory of Radionuclides Pollution Control and Resources, Guangzhou, 510006, China
[d] Department of Earth Sciences, University of Oxford, Oxford, OX1 3AN, UK
[e] College of Resources and Environmental Sciences, China Agricultural University, Beijing, 100193, China
[f] Department of Geosciences, National Taiwan University, Taipei, 10617, Taiwan
[g] Research Center for Future Earth, National Taiwan University, Taipei, 10617, Taiwan
[h] College of Chemistry and Chemical Engineering, Shaoxing University, Shaoxing, 312000, China
[i] School of Life & Environmental Science, Wenzhou University, Wenzhou, 325027, China

ARTICLE INFO

Article history:
Received 24 June 2018
Received in revised form
24 September 2018
Accepted 3 October 2018
Available online 9 October 2018

Keywords:
Uranium
Uranium mill tailings
Leaching test
Acid rain

ABSTRACT

To date, there is not sufficient knowledge to fully understand the occurrence, transport and fate of residual uranium (U) from uranium mill tailings (UMT). Herein this study investigated different U release behaviors from natural UMT (without grinding) under four simulated acid rain (pH = 2.0–5.0) compared with controlled scenario (pH = 6.0) for 25 weeks. The results showed that the most notable U release was observed from $UMT_{pH2.0}$, followed by $UMT_{pH3.0}$ whereas a nonlinear relationship between pH and U release was observed from $UMT_{pH4.0–6.0}$. The divergence of U release behaviors was attributed to the presence of minerals such as calcite and clinochlore. Autunite, a secondary mineral formed after leaching, might regulate U release in $UMT_{pH3.0–6.0}$. Fick theory model revealed the shift of U release mechanism from surface dissolution to diffusion transport for $UMT_{pH2.0}$, $UMT_{pH3.0}$ and $UMT_{pH5.0}$ at varied stage, whereas $UMT_{pH4.0}$ and $UMT_{pH6.0}$ displayed univocal dissolution and diffusion mechanism, respectively. This study highlights the necessity of performing long-term leaching tests to detect the "shift event" of leaching kinetics and to better understand the mechanism of U release influenced by mineralogy of the natural UMT under simulated acid rain conditions, which is conducive to developing UMT management strategies to minimize the risk of U release and exposure.

© 2018 Elsevier Ltd. All rights reserved.

1. Introduction

Uranium (U) is a toxic and radioactive contaminant in the environment; there has been increasing number of studies focusing on the remediation of U contamination (Carter et al., 2009; Pan et al., 2016; Rufyikiri et al., 2006) and a variety of new methods of U removal have been developed in accordance (Gu et al., 2018; Han et al., 2018; Yin et al., 2017; Zhang et al., 2018). At the same time, U has become one of the world's most important energy materials in the last 60 years, accompanied with increasing U mining and processing activities (Fang et al., 2018; Ilankoon et al.,

☆ This paper has been recommended for acceptance by Dr. J Rinklebe.

* Corresponding author. School of Environmental Science and Engineering, Guangzhou University, Guangzhou 510006, China.
** Corresponding author. Innovation Center and Key Laboratory of Waters Safety & Protection in the Pearl River Delta, Guangzhou University, Guangzhou 510006, China.
E-mail addresses: wangjin@gzhu.edu.cn (J. Wang), juan.liu@earth.ox.ac.uk, liujuan@gzhu.edu.cn (J. Liu).

[1] These authors contributed equally to this publication.

https://doi.org/10.1016/j.envpol.2018.10.018
0269-7491/© 2018 Elsevier Ltd. All rights reserved.

2018). Uranium mill tailings (UMT) are the crushed ore residues from the extraction of U from ores such as pitchblende (Landa, 2004). Uranium mining and processing have been concomitant with the generation of huge amount of UMT. According to a previous estimate from Steinhausler and Zaitseva (2007), the total amount of UMT due to U mining worldwide is about 2352 million tones. These UMT often contain surprisingly high concentrations of residual U, thorium and other toxic metals (Robinson, 2004; Zhang et al., 2015), and usually have a much higher porosity and permeability than the ores from which they are derived (Ferry et al., 2002). In the past decades, it is not rare that UMT has been stacked on the land surface after simple treatment of lime neutralization. Some of the UMT are further treated with landfill cover with a variety of plants, vegetation or trees to enhance the conservation (Waugh et al., 2008).

However, the chemical and radioactive elements in UMT could be mobilized during long-term redox and weathering processes. The mobilization would be even more significant under acid condition as acidity is one of the most important factors influencing the release of toxic elements from solid wastes (Förstner, 1987). The acid condition could be achieved in UMT if sulfuric acid was used to dissolve the U from the ores. Except for ores having a high carbonate content, the commercial extraction of U from ores generally involves leaching with sulfuric acid (Landa, 2003). For most of U industries in China, sulfuric acid was also mainly adopted (Wang et al., 2012a). The acid condition could also be achieved due to oxidation of sulfidic minerals in the tailings; the extent of acid generation is dependent on the concentration of sulfide, which ranges from a few to tens of wt% in UMT (Abdelouas, 2006). The low pH condition could accelerate the release of radioactive and hazardous elements from UMT. Consequently, the residual U and other metals in the UMT can release into ambient environment, and thus UMT may become a substantial source of surface and groundwater contamination (Liu et al., 2017; Liu et al., 2015; Wang et al., 2016). The release would be greatly enhanced if suffered from the local acid rain. Many studies have demonstrated the significant effect of pH on U release from various materials (Mason et al., 1997; Xu et al., 2004; Zhang and Wang, 2017). Nevertheless, few studies have examined the behaviors and mechanisms of U mobilization from natural UMT (without grinding). Although general leaching characteristics can be identified in leaching studies using U tailings ground before leaching, identifying and quantifying the natural processes of exposure of U-containing minerals to long-term weathering and corrosion remains a substantial challenge. To date, the knowledge about natural UMT hazards in the light of long-term leaching studies is limited, which however is essential for the development of sound UMT management strategies.

Semi-dynamic leaching tests are usually employed to elucidate the dominant leaching mechanism from a solid waste in which the leaching agent is renewed periodically (Kosson, 2002). Using this method, the present study investigated the release of U from the most common natural UMT. The leaching experiments were performed under simulated acid rain with pH ranging from 2.0 to 5.0 and a simulated normal rain for comparison. The objectives of this study were (i) to quantify the long-term U leaching characteristics from natural UMT influenced by acid rain, (ii) to unravel the mobilization mechanism based on mineralogy and kinetics evidences, and (iii) to inform the prospects for remediating U contamination from UMT.

2. Materials and methods

2.1. UMT sampling

The U metallogenic province in South China is the largest known deposit of U in China (Luo et al., 2017). Previous studies have revealed that the granite hosted U ore deposits provide ~30% of the U production in China during the past three decades (Hu et al., 2008; Hu et al., 2009; Luo et al., 2015; Wang et al., 2017b). The determined U concentration in the fine ore was 10957 ± 13 mg/kg, and the reported grade (% U) of the granite hosted U ore deposit in China is 0.1–1 (Dahlkamp, 2009), which shares the same order of magnitude. The natural UMT (without grinding) used in this study were collected from an unrehabilitated tailings dam where huge amount of UMT were piled near a large U hydrometallurgy plant in Guangdong Province, South China. The freshly disposed UMT with slightly wet surface were sampled using a wooden shovel, stored in a large plastic box, and were then air dried prior to semi-dynamic leaching tests. The grain size of the UMT selected for this study were between 6 and 10 mm, which is the dominant size fraction of the UMT. The U concentration in this fraction of the UMT was 997.9 ± 52.6 mg/kg. The concentrations of some other closely related elements were shown as follows: P (0.07%), K (3.3%), Mg (0.6%), Na (1.7%), Fe (2.0%), Al (6.9%) and Ca (0.7%).

2.2. Semi-dynamic leaching test

To investigate the long-term fate of U in UMT during the intermittent leaching and weathering process, five sets of semi-dynamic leaching tests with simulated acid rain and normal rain were carried out. Before the leaching test, UMT was washed with deionized water three times to remove the surface-adhered salts. The five leaching tests with pH ranging from 2.0 to 6.0 with a total duration of 25 weeks, were then conducted as follows. Leaching experiments were carried out in five brinell funnels (20 cm in diameter) each loaded with 1 kg of UMT. In each leaching cycle, the five UMT loaded brinell funnels were sprayed slowly with a plastic watering pot, which resembled the rainfall precipitation process. 800 mL of the simulated rain was used in each brinell funnel, which could just inundate the UMT's surface. Deionized water acidified by sulfuric acid (trace metal grade) to pH 2.0, 3.0, 4.0 and 5.0 were used as simulated acid rain, whereas deionized water (pH ~6.0) was used as simulated normal rain for comparison. The deionized water was produced by Milli-Q System (Millipore, Bedford, USA), and no additional treatment was used. After soaking for 1 h, the leachate was recovered for physico-chemical analysis, and the UMT in the brinell funnels was exposed to the air for the rest of the week until next leaching cycle commenced. The leachants were renewed in each cycle. The semi-dynamic leaching events were carried out once every 7 days and lasted for 25 weeks. The experiments were performed in open system to ensure good simulations of the natural weathering conditions for the UMT. The five sets of semi-dynamic leaching tests were performed simultaneously, and were referred to hereafter as $UMT_{pH2.0}$, $UMT_{pH3.0}$, $UMT_{pH4.0}$, $UMT_{pH5.0}$ and $UMT_{pH6.0}$, respectively.

After each leaching cycle, the leachate was drained into 1000 mL beaker. After settlement for 2 min, the supernatants were filtered to 0.45 μm using nylon syringe filters. The pH, redox potential (ORP) and conductivity (EC) of the filtered leachate were measured immediately after collection. The rest of the filtered leachate was acidified to 1% HNO_3 (trace metal grade), and stored at 4 °C until analysis for solution composition. UMT before and after 25 week leaching were collected and used for mineralogical and morphological characterizations by X-ray diffraction (XRD), scanning electron microscope and energy dispersive spectrometer (SEM-EDS), transmission electron microscope and energy dispersive X-ray spectrometry (EDS) in scanning TEM (TEM/STEM-EDS), Fourier-transform infrared spectroscopy (FTIR) and sequential extraction.

2.3. Analytical methods for the leachate

pH and redox potential of the leachate were measured simultaneously using a calibrated redox potential-acidity meter (PB-10, Sartorius, Inc., Germany), and EC was measured using a calibrated conductivity meter (ECTestr11^{+}, Eutech Instruments, Inc., USA). Dissolved U concentration in the leachate was determined by inductively coupled plasma mass spectrometry (ICP-MS, Elan 6100 DRC-e, PerkinElmer, Inc., USA). Each sample was run three times and averaged. Accuracy was verified against known quality controls. The standard deviations of three runs were less than 5%. Dissolved concentrations of other elements were determined by inductively coupled plasma optical emission spectroscopy (ICP-OES, Optima 7000 DV, PerkinElmer, Inc., Waltham, USA).

2.4. Analytical methods for UMT

2.4.1. XRD

XRD was used to assess UMT bulk mineralogy. To conduct XRD analysis, the air dried UMT samples were ground to powder with an average particle diameter smaller than 5 μm using an agate mortar-and-pestle set, and then mounted on a titanium aluminide-alloy test block. XRD patterns were collected using a PANalytical X'Pert Pro diffractometer (The Netherlands). The diffractometer used Cu Kα radiation ($\lambda = 1.5406$ Å) and scanned over 2θ range from 5° to 80°, with a step size of 0.02° and a counting time of 150 s per step. The identification search match of the various minerals were obtained using MDI Jade 5.0 equipped with the JCPDS PDF-2 database.

2.4.2. SEM-EDS

SEM-EDS was used to assess the morphology and composition of the pre- and post-leaching UMT powder. To avoid the charging effect on the sample surface, the samples were sputter coated with platinum (Pt) using an ion-sputtering coater equipment (HITACHI E−1045). The morphology was then recorded by a field emission scanning electron microscope (FESEM, SU8010, Hitachi, Japan) at 1.5 kV accelerating voltage and a working distance (WD) of 5.0 mm. Meanwhile, the elemental composition of selected spots on the specimens were determined by energy dispersive spectrometer (EDS).

2.4.3. TEM/STEM-EDS

Post-leaching UMT powder was dispersed in alcohol for 5 min, and then was deposited onto a carbon-coated copper grid, which was left to stand for 10 min prior to being analyzed by a 200 kV JEOL JEM-2100 high-resolution transmission electron microscope. The distribution and concentrations of targeted elements in representative particles from post-leaching UMT were determined by STEM-EDS, and the U-containing minerals were identified using selected-area electron diffraction (SAED) patterns.

2.4.4. FT-IR

Pre- and post-leaching UMT powder were dispersed in KBr by compression to form a sheet, and then the FT-IR spectra were collected using a Fourier transform infrared spectroscopy (Tensor 27, Bruker, Germany) with the wavenumber range of 400−4000 cm^{-1} and resolution of 0.4 cm^{-1}.

2.4.5. Sequential extraction

Sequential extraction was used to determine the chemical speciation of U in pre-leaching UMT. The sequential extraction procedure was based on a modified BCR procedure recommended by IRMM (Institute for Reference Materials and Measurement, Europe). The procedure included three successive steps to distinguish different pools of U: (i) a 16 h acetic acid (HOAc, 0.11 M, pH 2.8) extraction targeting exchangeable and acid-extractable U, (ii) a 16 h hydroxylamine-hydrochloride ($NH_2OH{\cdot}HCl$, 0.5 M, pH 1.5) extraction targeting reducible U, and (iii) a 16 h hydrogen peroxide/ammonium oxalate (8.8 M H_2O_2/1.0 M NH_3OAc, pH 2.0) extraction targeting oxidizable U. Extractions were conducted with a dry mass of 0.5 g and an extractant volume of 20 mL (25 mL for NH_3OAc), at room temperature in constantly agitated polyethylene centrifuge tubes. At the end of each extraction step, suspensions were centrifuged. The supernatants were then filtered to 0.2 μm and analyzed by ICP-MS as described above, and solids were treated with the next extractant. The residual fraction after extractions was digested with HNO_3-HF-$HClO_4$ (trace metal grade) and analyzed accordingly.

2.4.6. Fick theory model

The mechanism of U release can be depicted by the slope of the linear regression of the logarithmic of cumulative flux against leaching time (Torras et al., 2011). When the slope is > 0.65, the release of U is dominated by mineral dissolution; when the slope is between 0.35 and 0.65 (including 0.65), the release of U is dominated by diffusion transport; and when the slope is ≤ 0.35, the release of U is dominated by surface wash-off. The cumulative flux ($B_{ac\ i}$) was calculated based on previously published procedures (Wang et al., 2012b).

3. Results and discussion

3.1. The nonlinear effects of leaching pH

Dissolved concentration of U and leachate pH from the semi-dynamic leaching tests are presented in Fig. 1, where four simulated acid rain and one simulated normal rain were compared. While low leachate pHs were observed in $UMT_{pH2.0}$ and $UMT_{pH3.0}$, the leachate pHs of $UMT_{pH4.0}$ and $UMT_{pH5.0}$ were overall higher than the corresponding leachants, indicating the UMT has a noticeable pH buffering capacity. Such pH buffering capacity is usually owing to the presence of natural minerals that have prominent proton adsorption capacity under acidic environments, including calcite, smectite, allophane, illlite, chlorite, kaolinite, vermiculite and Fe, Al-oxides (Szecsody et al., 2013). Among these minerals, calcite and chlorite existed in significant quantities in our experiments, based on XRD results (Fig. 2). Compared to chlorite, the dissolution of calcite typically results in much more significant increase of leachate pH (Szecsody et al., 2013). Accordingly, the relatively rapid rise of leachate pH from $UMT_{pH4.0}$, $UMT_{pH5.0}$ and $UMT_{pH6.0}$ in some leaching periods might be predominantly attributed to the dissolution of calcite. It is important to note that the sharp fluctuation of leachate pH until the 13th week and definite pH decrease at the later stage in $UMT_{pH6.0}$, reflected the opposite impacts on pH from the dissolution of alkaline minerals and the oxidation of sulfide substance, which later prevailed.

Dissolved U concentrations in the leachate during the 25-week semi-dynamic leaching tests overwhelmingly exceeded 50 μg/L in $UMT_{pH2.0}$ and $UMT_{pH3.0}$ and also occasionally exceeded 50 μg/L in $UMT_{pH4.0–6.0}$ (Fig. 1), the limit of Regulations for Radiation and Environmental Protection of Uranium Mining and Metallurgy (GB23727-2009) in China, not to mention the proposed guideline range initiated by the World Health Organization (WHO) (2−15 μg/L). Surprisingly, the leachate U concentrations in $UMT_{pH4.0}$ were lower than those in $UMT_{pH5.0}$ and close to those in $UMT_{pH6.0}$, suggesting a nonlinear relationship between the extent of U release and leaching pH.

The cumulative amount of U release from $UMT_{pH2.0}$ after 25 weeks was 328.8 mg/kg which exceeded that of $UMT_{pH3.0}$, $UMT_{pH4.0}$, $UMT_{pH5.0}$ and $UMT_{pH6.0}$ by a factor of 85, 590, 211 and

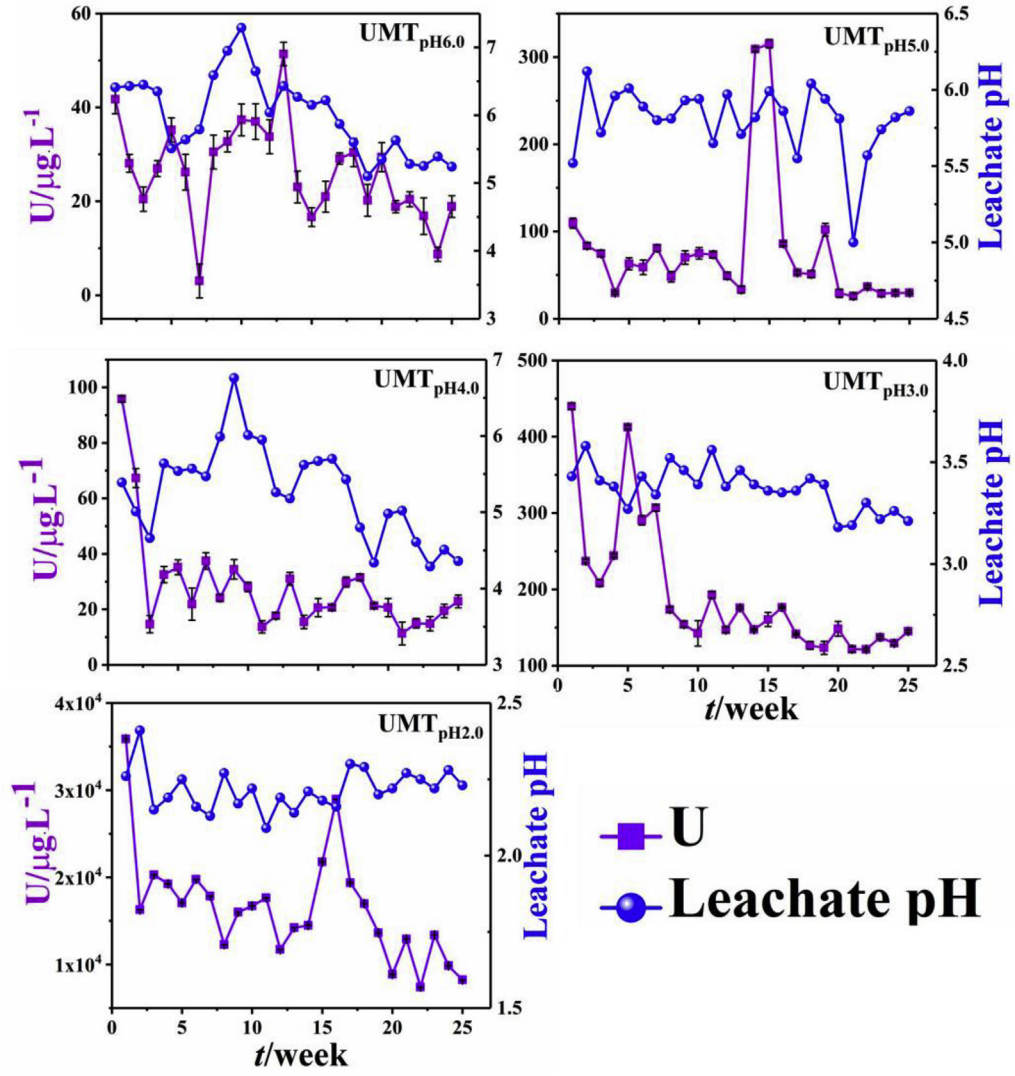


Fig. 1. Variations of leachate pH and dissolved U concentration versus leaching time.

625, respectively (Fig. 3). Leaching with simulated strong acid rain (pH = 2.0) resulted in the direct dissolution of U-bearing minerals and also the dissolution of some other minerals that suppress U adsorption by enhancing ionic strength and changing sorption surfaces (Szecsody et al., 2013). In fact, under such strong acid condition, U exists in the predominant form of uranyl cation with strong solubility (Szecsody et al., 2013) and cannot be adsorbed (Zachara et al., 2007). UMT$_{pH3.0}$, UMT$_{pH4.0}$, UMT$_{pH5.0}$ and UMT$_{pH6.0}$ showed a relatively low U concentration in the leachate, which could be in part attributed to a decrease of U solubility under leachate pH ranging from 3.18 to 7.29. Moreover, the subsequent precipitation of non-U minerals, *e.g.*, strengite, dolomite, diaspore and ferrihydrite would be feasible, which could coat the mineral surfaces and retard U mobilization (Szecsody et al., 2013).

Notably, the UMT displayed sustained U release in the leaching test. The cumulative amount (q_t) of extractable U versus leaching time increased rapidly in UMT$_{pH2.0}$ and UMT$_{pH3.0}$ while that in UMT$_{pH4.0}$ and UMT$_{pH6.0}$ increased slowly, as shown in Fig. 3. UMT$_{pH5.0}$ basically showed the same trend as UMT$_{pH4.0}$ except for the 14th and 15th weeks, during which an abrupt U release phenomenon was observed. The abrupt U release might be attributed to the stronger heterogeneity of natural UMT compared to ground tailings and the unsystematic exposure of U-containing minerals during leaching. Usually, the lower the pH of leachant, the higher the cumulative U release is expected. However, there was not a simple correlation between the leaching pH and the U release capability, highlighting the intricacy in mineral-solution geochemistry of UMT with relatively moderate pH leachants.

3.2. Complex leaching behavior controlled by different minerals

The XRD patterns of UMT before and after leaching were measured and compared, which is crucial for the interpretation of U release. The predominant mineral in UMT is quartz (SiO_2), followed by clinochlore ($Mg_5Al_2Si_3O_{10}(OH)_8$), lepidolite ($KMg_3AlSi_3O_{10}OHF$), and albite ($NaAlSi_3O_8$). It is worth noting that clinochlore existed in considerable amounts in both pre- and post-leaching UMT, while the comparatively high amount of calcite was only observed in pre-leaching UMT. Calcite was expected to play a vital role in the migration of U from UMT (Kipp et al., 2009), since the dissolution of calcite due to acidification might lead to liberation of soluble uranyl ion, owing to the formation of solution complexes between uranyl ion and anions such as carbonate, phosphate and sulfate under acidic conditions. The absence of calcite in post-leaching UMT was corroborated from XRD patterns, which might have contributed to the release of carbonates-bound U

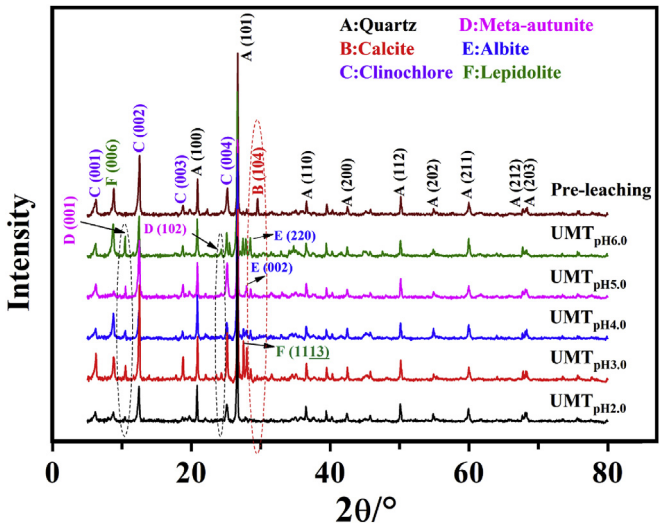


Fig. 2. XRD patterns of pre- and post-leaching UMT. B(104) denotes calcite, which was only observed in pre-leaching UMT. D(001) and D(102) are attributed to meta-autunite, a secondary mineral, which were not observed in pre-leaching UMT and negligible in $UMT_{pH2.0}$.

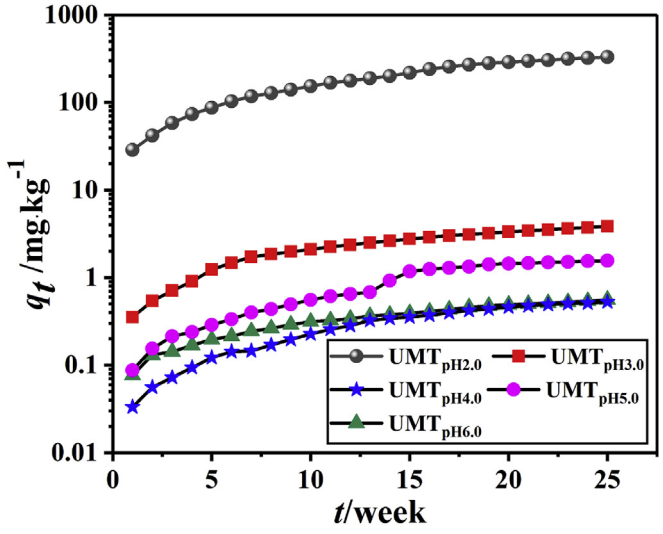


Fig. 3. The cumulative amount (q_t) of extractable U versus leaching time.

during the leaching test. Clay minerals, such as clinochlore, often have a high adsorption capacity for U, which however is exchangeable (Kim et al., 2016). Sequential extractions showed that pre-leaching UMT possessed remarkably high contents of exchangeable and acid-extractable U (60.46%, shown in Table 1). The reactions related to calcite and clinochlore could be deemed as the predominant mechanism of U release in the presence of simulated acid rain. It's also worth noting that, a U-bearing secondary mineral, *i.e.*, meta-autunite ($Ca(UO_2)_2(PO_4)_2 \cdot 3H_2O$) was observed merely in post-leaching UMT, suggesting the precipitation of new U-containing minerals only after UMT suffered from long-time intermittent leaching and weathering.

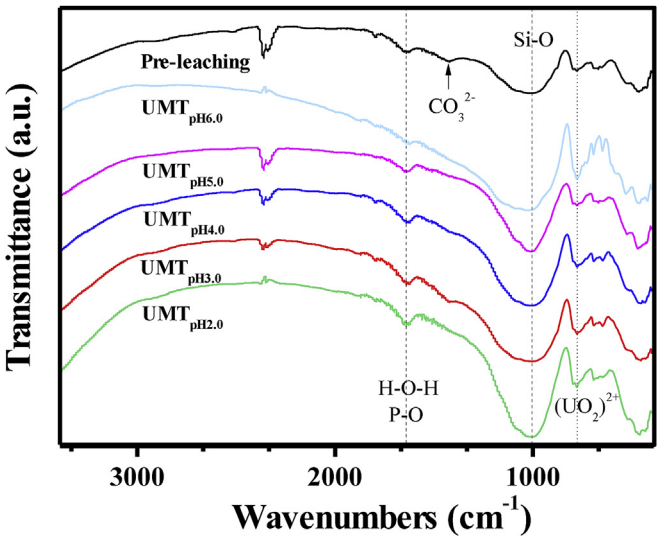


Fig. 4. FT-IR spectra of pre- and post-leaching UMT. Individual spectra are vertically offset for clarity.

SEM-EDS (Fig. S1) provided additional important information on the variations of morphology and elemental composition in the pre- and post-leaching UMT. A significant amount of $CaCO_3$ was found in pre-leaching UMT while was not observed in post-leaching UMT, which was in accordance with the XRD results. Provided the findings from SEM-EDS and XRD, more detailed and interesting features of the interactions between UMT and leachants were identified. The exhibited compact structure of pre-leaching UMT appeared to be different from the morphology of post-leaching UMT, indicating the corrosion of silicate after being leached and weathered for prolonged period. In addition, the concomitant increase of specific surface area may increase the rate of mineral dissolution but may also promote the re-adsorption of U on the mineral surface during solid-liquid equilibrium.

The FT-IR spectra of UMT before and after leaching help us to further understand the leaching mechanism (Fig. 4). A broad band at about 1435 cm^{-1} was presented in pre-leaching UMT, which can be assigned to carbonate ions, corresponding to calcite (Valente et al., 2012). This broad band was merely observed at pre-leaching UMT, confirming the complete dissolution of calcite after leaching, in good agreement with XRD and SEM-EDS results. Moreover, a shoulder peak at ~777 cm^{-1} was presented in all UMT, almost with no pH dependent spectral changes. This shoulder peak could be attributed to $(UO_2)^{2+}$ stretching vibration from uranophane ($Ca[UO_2]_2[SiO_3(OH)]_2 \cdot 5H_2O$) (Čejka, 1999). The weak peaks also from all UMT at around 1640 cm^{-1} were assigned to P-O and/or H-O-H (Günister et al., 2007; Zhou et al., 2014). The co-occurrence of stronger peaks/bands of P-O and/or H-O-H, $(UO_2)^{2+}$ and Si-O in the post-leaching UMT, relative to pre-leaching, suggested the possible formation of uranium-silicate/phosphate phases after 25 weeks of semi-dynamic leaching. These U-bearing secondary minerals could form under our experimental condition at room temperature (Nguyen et al., 1992). Such formation might also be partly the reason why the release of U from UMT slowed down at the later leaching stages.

Table 1
The content (average ± standard deviation) in mg kg^{-1} and portion (%) of U in specific geochemical fraction in the pre-leaching uranium mill tailings (UMT).

Geochemical fraction	Acid-extractable	Reducible	Oxidizable	Residual
U content (portion)	617.2 ± 3.1 (60.46%)	152.35 ± 3.5 (14.92%)	221.62 ± 4.2 (21.71%)	29.68 ± 1.9 (2.91%)

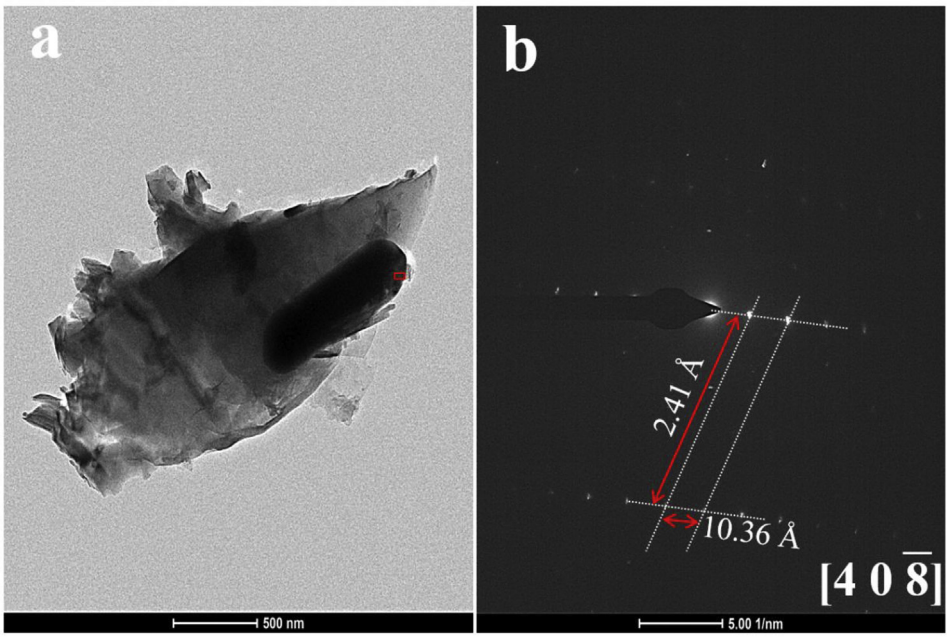


Fig. 5. TEM image and SAED pattern of a representative particle in post-leaching $UMT_{pH6.0}$, a) TEM image. b) SAED pattern of the [4 0$\bar{8}$] zone axis of autunite ($Ca(UO_2)_2(PO_4)_2 \cdot 11H_2O$) obtained from the red rectangle of a). (For interpretation of the references to colour in this figure legend, the reader is referred to the Web version of this article.)

TEM/STEM-EDS characterization was additionally conducted to identify the U-retaining phases in the example of $UMT_{pH6.0}$, shown in Fig. S2 and Fig. 5. Clearly, U was concentrated on a particle (prolate spheroid shape) while P and Ca were densely distributed on the same particle (Fig. S2). A selected-area electron diffraction (SAED) on the edge of this particle was conducted to unravel the phases that host U. The diffraction spots in the SAED pattern were obtained by the cast of [4 0$\bar{8}$] zone axis of autunite ($Ca(UO_2)_2(PO_4)_2 \cdot 11H_2O$), with *d*-spacing of ~10.36 Å and ~2.41 Å (Fig. 5b). Consistently, meta-autunite ($Ca(UO_2)_2(PO_4)_2 \cdot 3H_2O$), the product of autunite dehydration which emerged rapidly in semi-dynamic leaching condition (Sowder et al., 2000), was also identified by XRD in post-leaching UMT. The morphology and size of autunite particle were illustrated in the TEM image (Fig. 5a). The autunite particle was similar to a prolate spheroid with a length of ~1 μm, in which case U migration may be retarded by the effect of capillary barriers (Um et al., 2010). A previous spectroscopic study on the mechanism responsible for U release from sediments found that micrometer-sized metatorbernite ($Cu(UO_2)_2(PO_4)_2 \cdot 8H_2O$) and more soluble uranophane ($Ca[UO_2]_2[SiO_3(OH)]_2 \cdot 5H_2O$) were the U minerals that predominantly controlled U release during the interactions between waste discharge and sediments (Arai et al., 2007). Furthermore, the rapid precipitation of meta-ankoleite ($K(UO_2)(PO_4) \cdot 3H_2O$) was previously identified when sediments reacted with acidic U-bearing wastewater, and meta-ankoleite could easily be entrapped in sediments (Wang et al., 2017a). Likewise, autunite ($Ca(UO_2)_2(PO_4)_2 \cdot 11H_2O$) found in UMT in the present study could be a result of the long-term interaction between UMT and simulated acid rain, the formation of which is of significant importance for U immobilization.

3.3. Mechanism of uranium release revealed by the leaching kinetics

The data from the performed semi-dynamic leaching test could be well described by the Fick theory model, which allows the identification of the dominant leaching mechanism based on the slope of the linear regression of the logarithm of cumulative flux ($B_{ac\ i}$) versus time in logarithmic scale (Moon and Dermatas, 2006; Torras et al., 2011). As shown in Fig. 6, the leaching patterns for $UMT_{pH2.0}$, $UMT_{pH3.0}$ and $UMT_{pH5.0}$ were dominated by mineral dissolution in the beginning but turned to diffusion in the latter period. In other words, "shift event" of leaching mechanism occurred. In contrast, $UMT_{pH4.0}$ and $UMT_{pH6.0}$, both of which showed relatively low and weekly steady release of U, were governed by the same leaching mechanism during the whole leaching period. The mechanism was identified to be dissolution and diffusion in $UMT_{pH4.0}$ and $UMT_{pH6.0}$, respectively.

Dissolved U concentrations in leachate from $UMT_{pH2.0}$, $UMT_{pH3.0}$

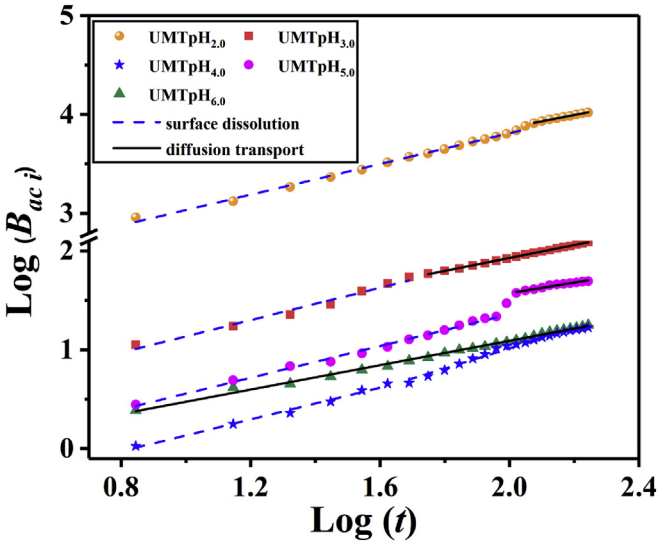


Fig. 6. Plot of log $B_{ac\ i}$ versus time to uncover U release mechanism from $UMT_{pH2.0}$, $UMT_{pH3.0}$, $UMT_{pH4.0}$, $UMT_{pH5.0}$ and $UMT_{pH6.0}$. The identification of release mechanism was showed by linear fit of log $B_{ac\ i}$ versus time, where solid line represents surface dissolution and dash line represents diffusion transport.

and $UMT_{pH5.0}$ were overall significantly higher than those from $UMT_{pH4.0}$ and $UMT_{pH6.0}$. The quick dissolution process triggered fast U release in the beginning stage of the leaching experiment, and lead to the formation of lots of microcrack on the UMT surfaces, as evidenced by the SEM images (Fig. S1). Therefore, it is possible that the rest of U reached saturation in porewaters inside the microcrack, thereafter U release would be dominated by a diffusion process. In addition, the diffusion of U from the inner porewaters was slower than the mineral dissolution at the leachant-UMT interface (Elkamash et al., 2006), which explains the slower U release in the latter leaching period.

4. Conclusions

In this study, the characteristics and mechanism of U release from natural U mill tailings (UMT) under simulated rain were unveiled by performing semi-dynamic leaching tests for 25 weeks and conducting complementary mineralogical analyses and modeling. The results showed clear differences in the rates and magnitudes of U release from UMT under different simulated acid/normal rain. The extent of U release from $UMT_{pH2.0}$ was significantly higher than the other tests, and the nonlinear relationship between leaching pH and the extent of U release was observed. The presence and dissolution of calcite and clinochlore in UMT are of crucial importance for explaining different U release behaviors under varied simulated acid/normal rain. Furthermore, autunite ($Ca(UO_2)_2(PO_4)_2 \cdot 11H_2O$) might form after intermittent leaching and weathering and regulated the further release of U in $UMT_{pH3.0–6.0}$. Fitting our experimental data with Fick theory model indicated that, U release was initially controlled by mineral dissolution and then by diffusion transport for $UMT_{pH2.0}$, $UMT_{pH3.0}$ and $UMT_{pH5.0}$, whereas dissolution and diffusion were the univocal release mechanism for $UMT_{pH4.0}$ and $UMT_{pH6.0}$, respectively.

This study highlights the necessity of carrying out long-term leaching tests to fully understand the mechanism of U release from UMT, because short-term leaching tests may not reveal the full picture due to shifts of kinetics influenced by geochemical weathering. Moreover, comprehending mineral composition of UMT has also shown to be important. For the studied UMT, U is predominantly bond to exchangeable and acid-extractable fraction, which has high release potential and therefore requires different management strategy from other UMT in which U is mainly entrapped in the residual, less reactive fraction. This study also suggested that the formation of U-bearing secondary mineral phases, *e.g.*, autunite ($Ca(UO_2)_2(PO_4)_2 \cdot 11H_2O$) is crucial for U immobilization when the UMT are exposed to intermittent leaching and weathering.

Acknowledgements

This work was jointly supported by the National Natural Science Foundation of China (No.41773011; 41501232; 41573008; 41873015; 41573119; U1612442), the Natural Science Foundation of Guangdong Province, China (2017A030313247; 2015A030313512), the Environmental Protection Ministry of Public Welfare Research Projects (201509051), Public Welfare Research Project of Zhejiang Province, China (LGF18E080013), and the Guangzhou University's 2017 training program for young top-notch personnel (BJ201709), and High Level University Construction Project of Guangdong Province (Regional Water Environment Safety and Water Ecological Protection). The Sponsorship from the China Scholarship Council (University of Oxford) granted to Jin Wang was acknowledged. The help from Dr. Jianying Qi from South China Institute of Environmental Sciences, Ministry of Ecology and Environmental with uranium measurement was highly appreciated.

Appendix A. Supplementary data

Supplementary data to this article can be found online at https://doi.org/10.1016/j.envpol.2018.10.018.

5. Notes

The authors declare no competing financial interest.

References

Abdelouas, A., 2006. Uranium mill tailings: geochemistry, mineralogy, and environmental impact. Elements 2, 335–341.
Arai, Y., Marcus, M.A., Tamura, N., Davis, J.A., Zachara, J.M., 2007. Spectroscopic evidence for uranium bearing precipitates in vadose zone sediments at the Hanford 300-area site. Environ. Sci. Technol. 41, 4633–4639.
Carter, M.L., Li, H., Zhang, Y., Vance, E.R., Mitchell, D.R.G., 2009. Titanate ceramics for immobilisation of uranium-rich radioactive wastes arising from 99Mo production. J. Nucl. Mater. 384, 322–326.
Čejka, J., 1999. Infrared spectroscopy and thermal analysis of the uranyl minerals. Rev. Mineral. Geochem. 38, 520–622.
Dahlkamp, F.J., 2009. China, people's republic of. In: Uranium Deposits of the World. Springer, Berlin, Heidelberg, pp. 1–26.
Elkamash, A.M., Elnaggar, M.R., Eldessouky, M.I., 2006. Immobilization of cesium and strontium radionuclides in zeolite-cement blends. J. Hazard Mater. 136, 310–316.
Förstner, U., 1987. Metal Speciation in Solid Wastes — Factors Affecting Mobility, pp. 11–41.
Fang, J., Chi, K.M.L., Lu, Z., Wu, W., 2018. Estimating peak uranium production in China – based on a stella model. Energy Pol. 120, 250–258.
Ferry, C., Richon, P., Beneito, A., Robé, M.C., 2002. Evaluation of the effect of a cover layer on radon exhalation from uranium mill tailings: transient radon flux analysis. J. Environ. Radioact. 63, 49–64.
Günister, E., Pestreli, D., Ünlü, C.H., Atıcı, O., Güngör, N., 2007. Synthesis and characterization of chitosan-MMT biocomposite systems. Carbohydr. Polym. 67, 358–365.
Gu, P., Zhang, S., Li, X., Wang, X., Wen, T., Jehan, R., Alsaedi, A., Hayat, T., Wang, X., 2018. Recent advances in layered double hydroxide-based nanomaterials for the removal of radionuclides from aqueous solution. Environ. Pollut. 240, 493–505.
Han, B., Zhang, E., Cheng, G., Zhang, L., Wang, D., Wang, X., 2018. Hydrothermal carbon superstructures enriched with carboxyl groups for highly efficient uranium removal. Chem. Eng. J. 338, 734–744.
Hu, R.Z., Bi, X.W., Zhou, M.F., Peng, J.T., Su, W.C., Liu, S., Qi, H.W., 2008. Uranium metallogenesis in South China and its relationship to crustal extension during the cretaceous to tertiary. Econ. Geol. 103, 583–598.
Hu, R.Z., Burnard, P.G., Bi, X.W., Zhou, M.F., Peng, J.T., Su, W.C., Zhao, J.H., 2009. Mantle-derived gaseous components in ore-forming fluids of the Xiangshan uranium deposit, Jiangxi province, China: evidence from He, Ar and C isotopes. Chem. Geol. 266, 86–95.
Ilankoon, I.M.S.K., Tang, Y., Ghorbani, Y., Northey, S., Yellishetty, M., Deng, X., Mcbride, D., 2018. The current state and future directions of percolation leaching in the Chinese mining industry: challenges and opportunities. Miner. Eng. 125, 206–222.
Kim, E., Ahn, H., Jo, H.Y., Ryu, J.H., Koh, Y.K., 2016. Chlorite alteration in aqueous solutions and uranium removal by altered chlorite. J. Hazard Mater. 327, 161.
Kipp, G.G., Stone, J.J., Stetler, L.D., Thompson, A., Vaughan, D.J., 2009. Arsenic and uranium transport in sediments near abandoned uranium mines in Harding County, South Dakota. Appl. Geochem. 24, 2246–2255.
Kosson, D.S., 2002. An integrated framework for evaluating leaching in waste management and utilization of secondary materials. Environ. Eng. Sci. 19, 159–204.
Landa, E.R., 2003. Mobilization of radionuclides from uranium mill tailings and related waste materials in anaerobic environments. J. Radioanal. Nucl. Chem. 255, 559–563.
Landa, E.R., 2004. Uranium mill tailings: nuclear waste and natural laboratory for geochemical and radioecological investigations. J. Environ. Radioact. 77, 1–27.
Liu, J., Luo, X., Wang, J., Xiao, T., Yin, M., Belshaw, N.S., Lippold, H., Kong, L., Xiao, E., Bao, Z.A., 2017. Provenance of uranium in a sediment core from a natural reservoir, South China: application of Pb stable isotope analysis. Chemosphere 193, 1172–1180.
Liu, J., Wang, J., Li, H., Shen, C.C., Chen, Y., Wang, C., Ye, H., Long, J., Song, G., Wu, Y., 2015. Surface sediment contamination by uranium mining/milling activities in South China. Clean. - Soil, Air, Water 43, 414–420.
Luo, J.C., Hu, R.Z., Fayek, M., Bi, X.W., Shi, S.H., Chen, Y.W., 2017. Newly discovered uranium mineralization at ~2.0 Ma in the Menggongjie granite-hosted uranium deposit, South China. J. Asian Earth Sci. 241–249.
Luo, J.C., Hu, R.Z., Fayek, M., Li, C.S., Bi, X.W., Abdu, Y., Chen, Y.W., 2015. In-situ SIMS uraninite U–Pb dating and genesis of the Xianshi granite-hosted uranium deposit, South China. Ore Geol. Rev. 65, 968–978.
Mason, C., Turney, W., Thomson, B., Lu, N., Longmire, P., Chisholmbrause, C., 1997.

Carbonate leaching of uranium from contaminated soils. Environ. Sci. Technol. 31, 2707–2711.
Moon, D.H., Dermatas, D., 2006. An evaluation of lead leachability from stabilized/solidified soils under modified semi-dynamic leaching conditions. Eng. Geol. 85, 67–74.
Nguyen, S.N., Silva, R.J., Weed, H.C., Jr, J.E.A., 1992. Standard Gibbs free energies of formation at the temperature 303.15 K of four uranyl silicates: soddyite, uranophane, sodium boltwoodite, and sodium weeksite. J. Chem. Thermodyn. 24, 359–376.
Pan, Z., Giammar, D.E., Mehta, V., Troyer, L.D., Catalano, J.G., Wang, Z., 2016. Phosphate-induced immobilization of uranium in hanford sediments. Environ. Sci. Technol. 50, 13486–13494.
Robinson, P., 2004. Uranium Mill Tailings Remediation Performed by the US DOE: an Overview. Southwest Research and Information Center, Albuquerque, NM.
Rufyikiri, G., Wannijn, J., Wang, L., Thiry, Y., 2006. Effects of phosphorus fertilization on the availability and uptake of uranium and nutrients by plants grown on soil derived from uranium mining debris. Environ. Pollut. 141, 420.
Sowder, A.G., Clark, S.B., Fjeld, R.A., 2000. Dehydration of synthetic autunite hydrates. International Journal for Chemical Aspects of Nuclear Science & Technology 88, 533–538.
Steinhausler, F., Zaitseva, 2007. Uranium mining and milling: material security and risk assessment. Int. J. Nucl. Govern. Econ. Ecol 1, 286–304.
Szecsody, J.E., Truex, M.J., Qafoku, N.P., Wellman, D.M., Tom, R., Lirong, Z., 2013. Influence of acidic and alkaline waste solution properties on uranium migration in subsurface sediments. J. Contam. Hydrol. 151, 155–175.
Torras, J., Buj, I., Rovira, M., De, P.J., 2011. Semi-dynamic leaching tests of nickel containing wastes stabilized/solidified with magnesium potassium phosphate cements. J. Hazard Mater. 186, 1954–1960.
Um, W., Icenhower, J.P., Brown, C.F., Serne, R.J., Wang, Z., Dodge, C.J., Francis, A.J., 2010. Characterization of uranium-contaminated sediments from beneath a nuclear waste storage tank from Hanford, Washington: implications for contaminant transport and fate. Geochem. Cosmochim. Acta 74, 1363–1380.
Valente, J.S., Rodriguez-Gattorno, G., Valle-Orta, M., Torres-Garcia, E., 2012. Thermal decomposition kinetics of MgAl layered double hydroxides. Mater. Chem. Phys. 133, 621–629.
Wang, G., Um, W., Wang, Z., Reinosomaset, E., Washton, N.M., Mueller, K.T., Perdrial, N., O'Day, P.A., Chorover, J., 2017a. Uranium release from acidic weathered hanford sediments: single-pass flow-through and column experiments. Environ. Sci. Technol. 51, 11011–11019.
Wang, J., Liu, J., Chen, Y., Song, G., Chen, D., Xiao, T., Li, H., Wang, C., Jiang, F., 2016. Preliminary results of spatial distribution of uranium and thorium in soil profiles near a uranium industrial site, Guangdong province, China. Nukleonika 61, 367–371.
Wang, J., Liu, J., Li, H., Chen, Y., Xiao, T., Song, G., Chen, D., Wang, C., 2017b. Uranium and thorium leachability in contaminated stream sediments from a uranium minesite. J. Geochem. Explor. 176, 85–90.
Wang, J., Liu, J., Li, H., Song, G., Chen, Y., Xiao, T., Qi, J., Zhu, L., 2012a. Surface water contamination by uranium mining/milling activities in northern Guangdong province, China. Acta Hydrochim. Hydrobiol. 40, 1357–1363.
Wang, J., Liu, J., Zhu, L., Qi, J.Y., Chen, Y.H., Xiao, T.F., Fu, S.M., Wang, C.L., Li, J.W., 2012b. Uranium and thorium leached from uranium mill tailing of Guangdong Province, China and its implication for radiological risk. Radiat. Protect. Dosim. 152, 215.
Waugh, W.J., Kastens, M.K., Sheader, L.R.L., Benson, C.H., Albright, W.H., Mushovic, P.S., 2008. Monitoring the Performance of an Alternative Landfill Cover at the Monticello, Utah, Uranium Mill Tailings Disposal Site, Paper Presented at: the Waste Management 2008; Conference, Phoenix 2008 February 24-28.
Xu, H., Wang, Y., Zhao, P., Bourcier, W.L., Van, K.R., Shaw, H.F., 2004. Investigation of pyrochlore-based U-bearing ceramic nuclear waste: uranium leaching test and TEM observation. Environ. Sci. Technol. 38, 1480.
Yin, L., Wang, P., Wen, T., Yu, S., Wang, X., Hayat, T., Alsaedi, A., Wang, X., 2017. Synthesis of layered titanate nanowires at low temperature and their application in efficient removal of U(VI). Environ. Pollut. 226, 125–134.
Zachara, J.M., Brown, C.F., Christensen, J.N., Davis, J.A., Dresel, P.E., Liu, C., Kelly, S.D., Mckinley, J.P., Serne, R.J., Um, W., 2007. A Site Wide Perspective on Uranium Geochemistry at the Hanford Site. Office of Scientific & Technical Information Technical Reports.
Zhang, B., Zhang, X.W., Mi, L.I., Tang, D.S., Jun-Wen, L.V., Tan, W.F., 2015. The Characteristics and Research Progress of Uranium Tailings Comprehensive Treatment Techniques. China Mining Magazine, pp. 58–62 in Chinese.
Zhang, C., Liu, Y., Li, X., Chen, H., Wen, T., Jiang, Z., Ai, Y., Sun, Y., Hayat, T., Wang, X., 2018. Highly uranium elimination by crab shells-derived porous graphitic carbon nitride: batch, EXAFS and theoretical calculations. Chem. Eng. J. 406–415.
Zhang, W., Wang, J., 2017. Leaching performance of uranium from the cement solidified matrices containing spent radioactive organic solvent. Ann. Nucl. Energy 101, 31–35.
Zhou, L., Jia, Y., Peng, J., Liu, Z., Al-Zaini, E., 2014. Competitive adsorption of uranium(VI) and thorium(IV) ions from aqueous solution using triphosphate-crosslinked magnetic chitosan resins. J. Radioanal. Nucl. Chem. 302, 331–340.